

## CMS constraints on the Higgs boson width from off-shell production and decay to Z-boson pairs

Loïc Quertenmont

on behalf of the CMS Collaboration

CP3, Université Catholique de Louvain, Belgium

### Abstract

We present the constraints set by the CMS collaboration on the total width of the recently discovered Higgs boson,  $\Gamma_H$ , using its relative on-shell and off-shell production and decay rates to a pair of Z bosons. The analysis is based on the data collected by the CMS experiment at the LHC in 2011 and 2012, corresponding to integrated luminosities of  $5.1 \text{ fb}^{-1}$  at a centre-of-mass energy  $\sqrt{s} = 7 \text{ TeV}$  and  $19.7 \text{ fb}^{-1}$  at  $\sqrt{s} = 8 \text{ TeV}$ . An upper limit on the Higgs boson width of  $\Gamma_H < 22 \text{ MeV}$  at a 95% confidence level was set using the  $ZZ \rightarrow 4\ell$  and  $2l2\nu$  final states. This bound corresponds to 5.4 times the expected value in the standard model at the measured mass of  $m_H = 125.6 \text{ GeV}$ .

*Keywords:* Higgs, Width, CMS, LHC, off-shell, boson, properties

### 1. Introduction

Both the CMS and ATLAS collaborations reported the discovery of a new boson of mass ( $m_H$ ) around 125 GeV [1, 2, 3]. The spin-parity properties of the new boson, studied by both experiments [4, 5, 6, 7], are consistent with the standard model (SM) Higgs boson. The observed signal was found consistent with a single narrow resonance and a direct upper limit of 3.4 GeV at a 95% confidence level (CL) on the new boson width ( $\Gamma_H$ ) has been reported by the CMS experiment. With the currently available data, the sensitivity for a direct width measurement at the resonance peak is therefore far beyond the expected width for the SM Higgs boson of about 4 MeV.

A new technique to constrain the Higgs boson width was recently proposed [8]. It relies on the off-shell Higgs boson production and decay to ZZ away from the resonance.

The contribution from off-shell production cross section to the total production cross section is known to be of the order of 8% for  $\sqrt{s} = 8 \text{ TeV}$ . It can even be enhanced up to about 20% when a kinematical selection is

used to extract the signal in the resonant region is taken into account [9, 10].

The gluon fusion production cross section as a function of  $m_{ZZ}$  can be written as:

$$\frac{d\sigma_{gg \rightarrow H \rightarrow ZZ}}{dm_{ZZ}^2} \sim \frac{g_{ggH}^2 g_{HZZ}^2}{(m_{ZZ}^2 - m_H^2)^2 + m_H^2 \Gamma_H^2} \quad (1)$$

where  $g_{ggH}$  and  $g_{HZZ}$  are the couplings of the Higgs boson to gluons and Z bosons, respectively. Integrating either in a small region around  $m_H$ , or above the mass threshold  $m_{ZZ} \geq 2m_Z$ , where the term depending on  $\Gamma_H^2$  can be neglected, the cross sections are, respectively,

$$\sigma_{gg \rightarrow H \rightarrow ZZ}^{\text{on-shell}} \sim \frac{g_{ggH}^2 g_{HZZ}^2}{m_H \Gamma_H} \quad (2)$$

$$\sigma_{gg \rightarrow H^* \rightarrow ZZ}^{\text{off-shell}} \sim \frac{g_{ggH}^2 g_{HZZ}^2}{(2m_Z)^2} \quad (3)$$

The ratio of Eq.(2) and Eq.(3) provides direct information on  $\Gamma_H$  under the assumption that the coupling ratios remain unchanged or can be estimated. In the rest of this document, the coupling ratio is as predicted by the standard model.

The dominant contribution for the production of a pair of Z bosons comes from the quark-initiated process,  $q\bar{q} \rightarrow ZZ$ , the diagram for which is displayed in Fig. 1(left). The gluon-induced diboson production involves the  $gg \rightarrow ZZ$  continuum background production from the box diagrams, as illustrated in Fig. 1(center). An example of the signal production diagram is shown in Fig. 1(right). The large interference [11] between the box and the signal diagrams in the off-shell region is taken into account in the analysis.

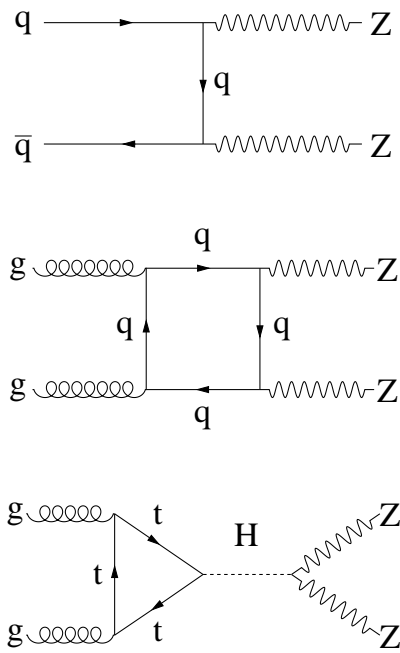


Figure 1: Lowest order contributions to the main ZZ production processes: (top) quark-initiated production,  $q\bar{q} \rightarrow ZZ$ , (middle)  $gg$  continuum background production,  $gg \rightarrow ZZ$ , and (bottom) Higgs-mediated  $gg$  production,  $gg \rightarrow H \rightarrow ZZ$ , the signal.

In the rest of this document we focus on summarizing the analyses of the off-shell Higgs boson production performed by CMS [12] in the  $ZZ \rightarrow 4\ell$  and  $ZZ \rightarrow 2\ell 2\nu$  final states. The study of the on-shell Higgs boson production, performed in the  $ZZ \rightarrow 4\ell$ , will not be described in this proceeding since it is identical to what is reported in Refs. [1, 2, 3].

## 2. Off-shell Higgs analysis in a nutshell

The analysis performed in both the  $4\ell$  and  $2\ell 2\nu$  final states are based on the same event reconstruction and

event selection as used in Refs. [7, 13]. The signal candidates are selected using well-identified and isolated prompt leptons. The CMS detector [14], provides excellent resolution for the measurement of electron and muon transverse momenta ( $p_T$ ) over a wide range.

The final state in the  $4\ell$  channel is characterized by four well-identified and isolated leptons forming two pairs of opposite-sign and same-flavour leptons consistent with two Z bosons. The off-shell signal is identified based on the four-lepton invariant mass distribution as well as a matrix element likelihood discriminant to separate the ZZ components originating from gluon- and quark-initiated processes. The off-shell signal region is selected by  $m_{4\ell} > 220$  GeV, on the contrary, the on-shell signal region is defined as  $105.6 < m_{4\ell} < 140.6$  GeV. This channel benefits from a precise reconstruction of all final state leptons and from a very low instrumental background. The event selection and the reducible background evaluation are performed following the methods described in Ref. [7]. After the selection, the  $4\ell$  data sample is dominated by the quark-initiated  $q\bar{q} \rightarrow ZZ \rightarrow 4\ell$  ( $q\bar{q} \rightarrow 4\ell$ ) and  $gg \rightarrow 4\ell$  productions. In order to enhance the sensitivity to the  $gg$  production in the off-shell region, a likelihood discriminant  $\mathcal{D}_{gg}$  is further used. The  $4\ell$  invariant mass distribution in the off-shell signal region ( $m_{4\ell} > 220$  GeV) and for  $\mathcal{D}_{gg} > 0.65$  is shown on Fig. 2.

The final state in the  $2\ell 2\nu$  channel is characterized by two oppositely-charged leptons of the same flavour compatible with a Z boson, together with a large  $E_T^{\text{miss}}$  from the undetectable neutrinos. We require  $E_T^{\text{miss}} > 80$  GeV. The event selection and background estimation are performed as described in Ref. [13], with the exception that the jet categories defined in Ref. [13] are here grouped into a single category, i.e. the analysis is performed in an inclusive way. The presence of neutrino does not permit to separate on-shell and off-shell signal based on the invariant mass of the system. We therefore rely on the transverse mass distribution  $m_T$ ,

$$m_T^2 = \left[ \sqrt{p_{T,2\ell}^2 + m_{2\ell}^2} + \sqrt{E_T^{\text{miss}^2} + m_{2\ell}^2} \right]^2 - \left[ \vec{p}_{T,2\ell} + \vec{E}_T^{\text{miss}} \right]^2, \quad (4)$$

where  $p_{T,2\ell}$  and  $m_{2\ell}$  are the measured transverse momentum and invariant mass of the dilepton system, respectively. The missing transverse energy,  $E_T^{\text{miss}}$ , is defined as the magnitude of the transverse momentum imbalance evaluated as the negative of the vectorial sum of transverse momenta of all the reconstructed particles in the event. In the  $2\ell 2\nu$  channel, the off-shell signal region is defined as  $m_T > 180$  GeV. The  $m_T$  distribution in the off-shell signal region ( $m_T > 180$  GeV) is shown

on Fig. 3.

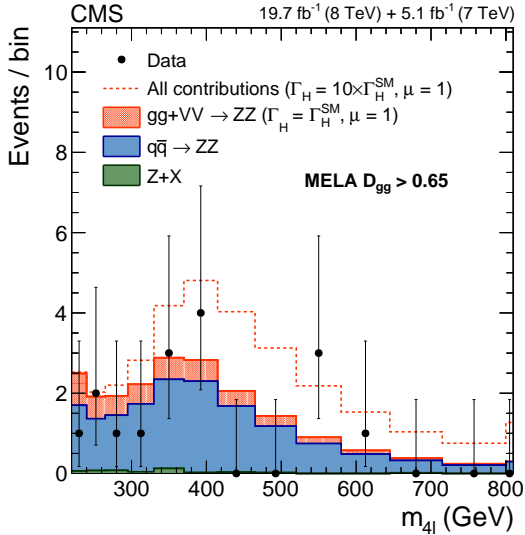


Figure 2: Distributions of the four-lepton invariant mass after a selection requirement on the MELA likelihood discriminant  $\mathcal{D}_{gg} > 0.65$ . Points represent the data, filled histograms the expected contributions from the reducible (Z+X) and  $q\bar{q}$  backgrounds, and from the gluon fusion (gg) and vector boson fusion (VV) SM processes (including the Higgs boson mediated contributions). The dashed line corresponds to the total expected yield for a Higgs boson width and a squared product of the couplings scaled by a factor 10 with respect to their SM values. The bin size varies from 20 to 85 GeV and the last bin includes all entries with masses above 800 GeV.

### 3. Statistical analysis and results

We perform a simultaneous unbinned maximum likelihood fit of a signal-plus-background model to the measured distributions in the  $4\ell$  and  $2\ell 2\nu$  channels. For the  $4\ell$  channel, both the on-shell and off-shell signal regions are considered. In the  $2\ell 2\nu$  channel, only the off-shell Higgs boson production is analyzed.

The probability distribution functions are built using the full detector simulation or data control regions, and are defined for the signal, the background, or the interference between the two contributions,  $\mathcal{P}_{\text{sig}}$ ,  $\mathcal{P}_{\text{bkg}}$ , or  $\mathcal{P}_{\text{int}}$ , respectively. Several production mechanisms are considered for the signal and the background, such as gluon fusion (gg), VBF, and quark-antiquark annihilation ( $q\bar{q}$ ).

The total Higgs width ( $\Gamma_H$ ), as well as the signal strengths in the gluon fusion ( $\mu_{\text{ggH}}$ ) and vector boson fusion ( $\mu_{\text{VBF}}$ ) production modes, are left unconstrained in the fit. The  $\mu_{\text{ggH}}$  and  $\mu_{\text{VBF}}$  fitted values are found to be almost identical to those obtained in Ref. [7]. The

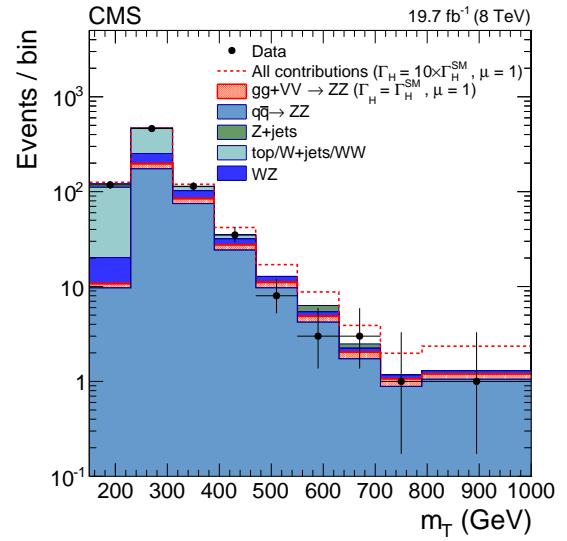


Figure 3: Distribution of the transverse mass in the  $2\ell 2\nu$  channel. Points represent the data, filled histograms the expected contributions from the backgrounds, and from the gluon fusion (gg) and vector boson fusion (VV) SM processes (including the Higgs-mediated contributions). The dashed line corresponds to the total expected yield for a Higgs boson width and a squared product of the couplings scaled by a factor 10 with respect to their SM values. The bin size varies from 80 to 210 GeV and the last bin includes all entries with transverse masses above 1 TeV.

fit results are shown in Fig. 4 as scans of the negative log-likelihood,  $-2\Delta \ln \mathcal{L}$ , as a function of  $\Gamma_H$ . Combining the two channels a limit is observed (expected) on the total width of  $\Gamma_H < 22$  MeV (33 MeV) at a 95% CL, which is 5.4 (8.0) times the expected value in the SM. The best fit value and 68% CL interval correspond to  $\Gamma_H = 1.8^{+7.7}_{-1.8}$  MeV.

### 4. Conclusion

In summary, the CMS collaboration has presented, in Ref. [12], constraints on the total Higgs boson width using its relative on-shell and off-shell production and decay rates to four leptons or two leptons and two neutrinos. The constraints are based on the assumption that the couplings ratio between on-shell and off-shell regions is as predicted by the SM. The analysis is based on the 2011 and 2012 data sets corresponding to integrated luminosities of  $5.1 \text{ fb}^{-1}$  at  $\sqrt{s} = 7 \text{ TeV}$  and  $19.7 \text{ fb}^{-1}$  at  $\sqrt{s} = 8 \text{ TeV}$ . The combined fit of the  $4\ell$  and  $2\ell 2\nu$  channels leads to an upper limit on the Higgs boson width of  $\Gamma_H < 22$  MeV at a 95% confidence level, which is 5.4 times the expected width of the SM Higgs boson.

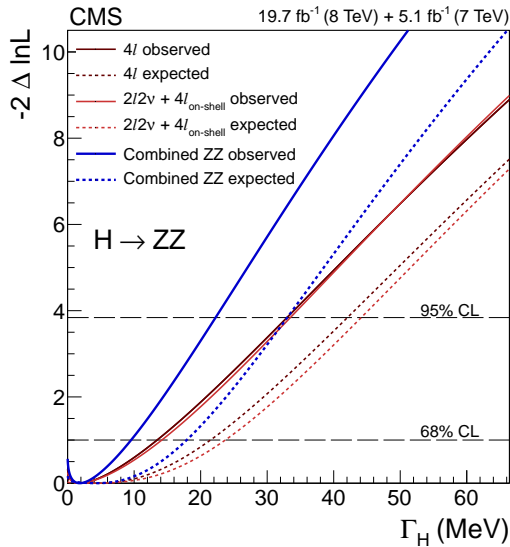


Figure 4: Scan of the negative log-likelihood,  $-2\Delta\ln\mathcal{L}$ , as a function of  $\Gamma_H$  for the combined fit of the  $4\ell$  and  $2\ell 2\nu$  channels (blue thick lines), for the  $4\ell$  channel alone in the off-shell and on-shell regions (dark red lines), and for the  $2\ell 2\nu$  channel in the off-shell region and  $4\ell$  channel in the on-shell region (light red lines). The solid lines represent the observed values, the dotted lines the expected values.

This result improves by more than two orders of magnitude upon previous experimental constraints on the new boson decay width from the direct measurement at the resonance peak.

As a last remark, I would like to highlight that this proceeding is only a short summary of this analysis. I would therefore recommend the interested reader to read the letter [12] that describes this analysis in greater details.

## References

- [1] G. Aad, et al., Observation of a new particle in the search for the Standard Model Higgs boson with the ATLAS detector at the LHC, *Phys. Lett. B* 716 (2012) 1. [arXiv:1207.7214](#), doi:10.1016/j.physletb.2012.08.020.
- [2] S. Chatrchyan, et al., Observation of a new boson at a mass of 125 GeV with the CMS experiment at the LHC, *Phys. Lett. B* 716 (2012) 30. [arXiv:1207.7235](#), doi:10.1016/j.physletb.2012.08.021.
- [3] S. Chatrchyan, et al., Observation of a new boson with mass near 125 GeV in pp collisions at  $\sqrt{s} = 7$  and 8 TeV, *JHEP* 06 (2013) 081. [arXiv:1303.4571](#), doi:10.1007/JHEP06(2013)081.
- [4] S. Chatrchyan, et al., Study of the Mass and Spin-Parity of the Higgs Boson Candidate via its Decays to Z Boson Pairs, *Phys. Rev. Lett.* 110 (2013) 081803. [arXiv:1212.6639](#), doi:10.1103/PhysRevLett.110.081803.
- [5] G. Aad, et al., Measurements of Higgs boson production and couplings in diboson final states with the ATLAS detector at

the LHC, *Phys. Lett. B* 726 (2013) 88. [arXiv:1307.1427](#), doi:10.1016/j.physletb.2013.08.010.

- [6] G. Aad, et al., Evidence for the spin-0 nature of the Higgs boson using ATLAS data, *Phys. Lett. B* 726 (2013) 120. [arXiv:1307.1432](#), doi:10.1016/j.physletb.2013.08.026.
- [7] CMS Collaboration, Measurement of the properties of a Higgs boson in the four-lepton final state, *Phys. Rev. D* 89 (2014) 092007. [arXiv:1312.5353](#), doi:10.1103/PhysRevD.89.092007.
- [8] F. Caola, K. Melnikov, Constraining the Higgs boson width with ZZ production at the LHC, *Phys. Rev. D* 88 (2013) 054024. [arXiv:1307.4935](#), doi:10.1103/PhysRevD.88.054024.
- [9] N. Kauer, G. Passarino, Inadequacy of zero-width approximation for a light Higgs boson signal, *JHEP* 08 (2012) 116. [arXiv:1206.4803](#), doi:10.1007/JHEP08(2012)116.
- [10] N. Kauer, Inadequacy of zero-width approximation for a light Higgs boson signal, *Mod. Phys. Lett. A* 28 (2013) 1330015. [arXiv:1305.2092](#), doi:10.1142/S0217732313300152.
- [11] G. Passarino, Higgs Interference Effects in  $gg \rightarrow ZZ$  and their Uncertainty, *JHEP* 08 (2012) 146. [arXiv:1206.3824](#), doi:10.1007/JHEP08(2012)146.
- [12] V. Khachatryan, et al., Constraints on the Higgs boson width from off-shell production and decay to Z-boson pairs, *Phys. Lett. B* 736 (2014) 64. [arXiv:1405.3455](#), doi:10.1016/j.physletb.2014.06.077.
- [13] S. Chatrchyan, et al., Search for a standard-model-like Higgs boson with a mass in the range 145 to 1000 GeV at the LHC, *Eur. Phys. J. C* 73 (2013) 2469. [arXiv:1304.0213](#), doi:10.1140/epjc/s10052-013-2469-8.
- [14] S. Chatrchyan, et al., The CMS experiment at the CERN LHC, *JINST* 3 (2008) S08004. doi:10.1088/1748-0221/3/08/S08004.